NASA TECHNICAL MEMORANDUM

NASA TM X-53663

October 17, 1967

NASA TM X-53663

WIND COMPARISON ANALYSIS OF PIBAL VERSUS ANEMOMETER

By Michael Susko
Aero-Astrodynamics Laboratory

NASA

George C. Marshall Space Flight Center, Huntsville, Alabama

TECHNICAL MEMORANDUM X-53663

WIND COMPARISON ANALYSIS OF PIBAL VERSUS ANEMOMETER

By

Michael Susko

George C. Marshall Space Flight Center

Huntsville, Alabama

ABSTRACT

The differences of lower atmosphere wind velocities obtained by a mast-mounted anemometer and 10-gram pilot balloons (pibals) are discussed. Wind velocity measurements were made by an anemometer mounted at the 15.24 meter level on a mast; whereas, simultaneous wind measurements were calculated from time referenced pibal photographs taken as the pibals passed the anemometer.

The absolute value of the mean difference in wind speed is 0.53 m sec^{-1} whereas the RMS value is 0.62 m sec^{-1}. The absolute value of the mean difference in wind direction is 4.9 degrees, while the RMS value is 5.6 degrees.

The data were obtained from forty experiments during 1966 and 1967 at the Marshall Space Flight Center, Huntsville, Alabama.

NASA - GEORGE C. MARSHALL SPACE FLIGHT CENTER

NASA - GEORGE C. MARSHALL SPACE FLIGHT CENTER

Technical Memorandum X-53663

October 17, 1967

WIND COMPARISON ANALYSIS OF PIBAL VERSUS ANEMOMETER

By

Michael Susko

ATMOSPHERIC DYNAMICS BRANCH
AEROSPACE ENVIRONMENT DIVISION
AERO-ASTRODYNAMICS LABORATORY
RESEARCH AND DEVELOPMENT OPERATIONS

ACKNOWLEDGEMENTS

The writer expresses his appreciation to personnel of the Atmospheric Research Facility, particularly Mr. Luke Gilcrist, for help in acquiring data, to Messrs. Elmer Fisher and Ernest Harden of the Technical Services Office, Photographic Branch, for photographic assistance, and to Messrs. John Kaufman, George Fichtl, and Robert Turner, of this Division, for their constructive suggestions.

TECHNICAL MEMORANDUM X-53663

WIND COMPARISON ANALYSIS OF PIBAL VERSUS ANEMOMETER

SUMMARY

The differences of lower atmosphere wind velocities obtained by a mast-mounted anemometer and 10-gram pilot balloons (pibals) are discussed. Wind velocity measurements were made by an anemometer mounted at the 15.24 meter level on a mast; whereas, simultaneous wind measurements were calculated from time referenced pibal photographs taken as the pibals passed the anemometer.

The absolute value of the mean difference in wind speed is 0.53 m sec^{-1}, whereas the RMS value is 0.62 m sec^{-1}. The absolute value of the mean difference in wind direction is 4.9 degrees, while the RMS value is 5.6 degrees.

The data were obtained from forty experiments during 1966 and 1967 at the Marshall Space Flight Center, Huntsville, Alabama.

I. INTRODUCTION

Low altitude wind information is of great importance in the design of the Saturn and other space vehicles. Interest in this subject is manifested by the articles in professional journals, technical reports, and other publications, as well as by the monetary support and scientific effort expended by government and private industry. Several comparisons of anemometer and pibal wind measurements have been made during recent years; particularly noteworthy is the work of Rider and Armendariz [1,2]. Some of the reasons for large wind differences between anemometer and balloon measured winds can be attributed to balloon aerodynamics, tower shadow effects, terrain effects, systems error and data reduction processes. It has been difficult to calculate the magnitude of these errors because of the unknown combinations of these factors.

This paper compares wind data obtained from tracking a 10-gram balloon with wind data obtained from a three-cup Climet anemometer (model 014) located on top of a 15.24-meter meteorological tower (for further details, see reference 3). After researching flight test data of 10-gram pibals of various diameters, it was determined that the 0.32-meter diameter pibal should be used because of its favorable aerodynamic properties.

II. DISCUSSION

A. Balloon Dynamics

One of the major factors which may contribute to the difference in wind measurements of the type under consideration is the size of the balloon. Other investigators have used the J-100 (100-gram balloon) which has a vertical rise rate of 5.03 m sec^{-1} and a diameter of 1.015 m*. The balloon operates approximately in the transition region between the unstable supercritical-turbulent region and stable subcritical-laminar flow where the Reynolds number, R, is on the order of $3 - 4 \times 10^5$. For an evaluation of the differences of the 100-gram pibal and tower wind profiles, see references 1 and 2.

The 10-gram pibal balloons operate within the laminar (smooth) region of the Reynolds number range on the order of $10^4 - 10^5$, and the drag coefficients C_D are on the order of 0.60 - 0.85.

Several preliminary flights were made to determine the optimum size of the 10-gram helium-inflated pibal. The pibal diameters considered were 0.24, 0.32, 0.40, and 0.48 m. The pibals were released so that the trajectory of the balloons would be as near as possible to the Climet 3-cup wind sensor on the top of the 15.24-meter meteorological tower. The total time it took the pibals to reach the 15.24-meter wind sensor was recorded.

Figure 1 shows the results of these 10-gram pibal tests. It should be noted that the pibal with a diameter of 0.24 meters never reached a height of 15.24 meters, at least, not under the conditions of this test day. Subsequently, the aerodynamic characteristics were calculated for the three 10-gram pibals (i.e., the 0.32, 0.40, and 0.48 meter diameter pibals) in addition to five other balloons of larger diameters. Table 1 shows the results of calculations in which the C_D and R are listed for the eight balloons with diameters ranging between 0.32 and 2.44 meters. Field tests of the balloons having a diameter of 1.22 meters and greater were conducted at Cape Kennedy, Florida, in 1963 (see reference 4).

Figure 2 and 3 show the aerodynamic characteristics of the eight balloons as discussed above. For purposes of comparison, the aerodynamic drag coefficients and the Reynolds numbers were calculated using the formula presented in appendix A (also, see references 4 and 5). In that the differences of the kinematic viscosity for Cape Kennedy (sea level) and MSFC, Huntsville, Alabama, (elevation $\sim$ 200 meters) is quite small, i.e., 1.46×10^{-5} and 1.48×10^{-5} m^2 sec^{-1}, respectively, as

*The J-100 gram balloon maintains a rise rate of about 5 m sec^{-1} to approximately 12 km [6].

calculated from the U. S. Standard Atmosphere, 1962 data, it is reasonable to combine the C_D and R values as presented.

Comparisons of C_D vs R for the above sphere diameters, as shown in table I, indicated that the pibal balloons with the smaller diameters were in the laminar flow region on the order of $R < 3 \times 10^5$. The large-diameter balloons (1.22, 2.00, 2.13, and 2.44 m) were in the transition and supercritical (turbulent) Reynolds number region on the order of $3 \times 10^5 - 10^6$. The 0.32 m diameter was chosen for the tower/pibal experiment because of its favorable aerodynamic properties, i.e., a Reynolds number of 0.31×10^5 and a drag coefficient of 0.82.

B. Data Reduction

Two 70 mm Hulcher cameras were positioned on a close-cropped, grassy field adjoining MSFC's Atmospheric Research Facility. The cameras were located 30.48 m south and east of the meteorological tower. The pibal winds were calculated by the outline in appendix B. The 70 mm cameras recorded the pibal position at 10 frames sec^{-1}, and the data were used to compute the balloon's position. At the instant the balloon reached the anemometer height, the operator triggered a light on the meteorological tower. This light or event marker was used to synchronize the data obtained from the tower anemometer and the pibal observations. The tower data were recorded on a strip chart that operates at a rate of 8 in min^{-1}. The trajectory of the balloon was computed at 1/2 - second averaging intervals centered around the time (event marker) at which the pibal reached the anemometer height. The event marker on the paper strip chart wind recorder was used to synchronize the wind speed and direction data with the pibal. At a chart advance rate of 8 inches per minute a 1/2 - second time period advances the chart about 1/16 of an inch. At this chart advance rate, and due to the response of the anemometer/wind recorder system, near instantaneous wind speeds and directions were read from the strip chart wind records. Subsequently, the pibal wind velocity data were compared.

C. Results

Wind direction and wind speed measurements are shown in table II. The wind direction and speed data of the tower-mounted anemometer and the pibal/balloon wind data are illustrated in the scatter diagrams shown in figures 4 and 5. The direction and wind speed generally follow the 1:1 correspondence line. The absolute value of the mean difference between the two sensors is 0.53 m sec^{-1}, while the RMS difference is 0.62 m sec^{-1}.

The range of the wind speed differences is -0.96 and +1.16 m sec^{-1}. The absolute value of the mean difference in wind direction is 4.9 degrees, while the RMS difference is 5.6 degrees. The range extends from -10 degrees to +9 degrees.

III. CONCLUSION

Differences of lower atmosphere wind velocities at the 15.24-meter level were obtained from a tower-mounted anemometer and a 10-gram pibal tracked by two 70 mm cameras. The field tests and aerodynamic calculations illustrate that the 10-gram pibal is the most favorable for low level wind measurements. The 10-gram pibal has a diameter of 0.32 m (1.05 ft) and rises at a rate of 1.62 m sec^{-1} (5.32 ft sec^{-1}). This balloon operates in the laminar flow region ($0.31 \times 10^5 < R$), and its drag coefficient is approximately 0.82. The absolute value of the mean differences in wind speed is 0.53 m sec^{-1} (1.74 ft sec^{-1}) and 4.9 degrees, respectively. The RMS value between the observations of the two wind sensors is 0.62 m sec^{-1} in wind speed (2.03 ft sec^{-1}) and 5.6 degrees in wind direction. These comparisons were conducted for anemometer wind velocities averaged over 1/2-second time periods for wind speeds ranges of 1 to 9 m sec^{-1}.

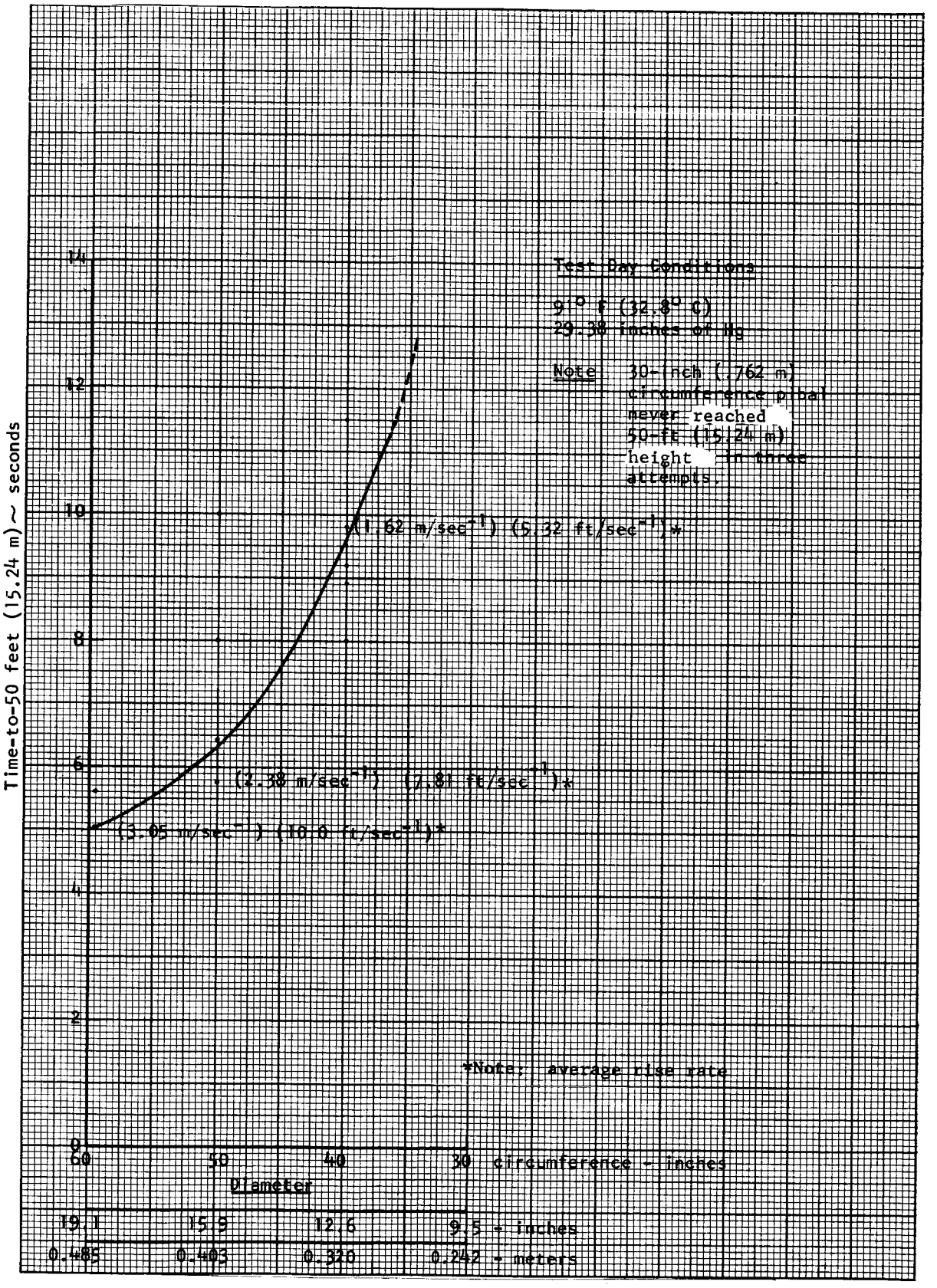

Figure 1. Ascent time of 10-gram pibal to 50 ft. (15.24 m) versus circumferences

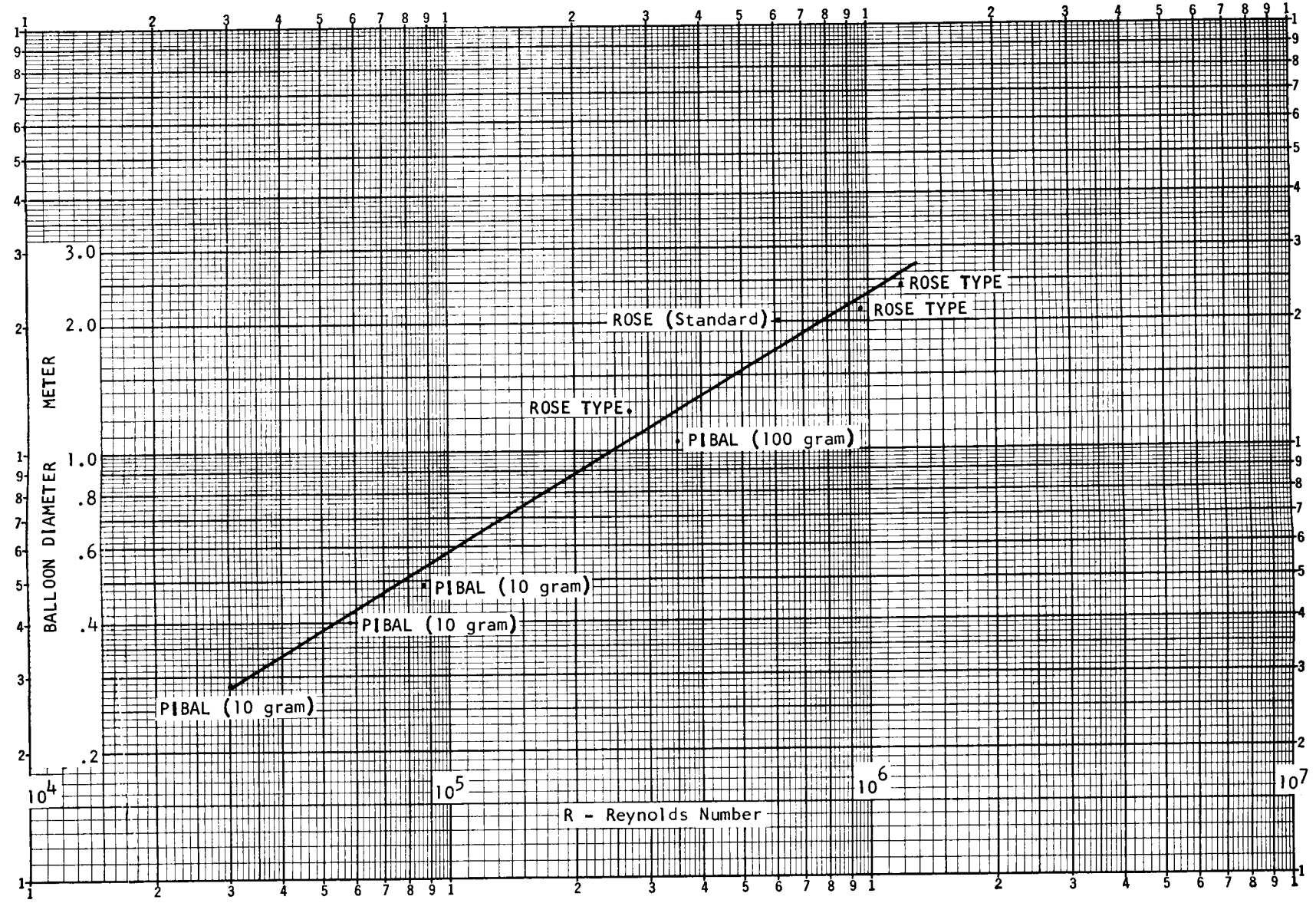

Figure 2. Reynolds Number (R) vs. Balloon Diameter (d)

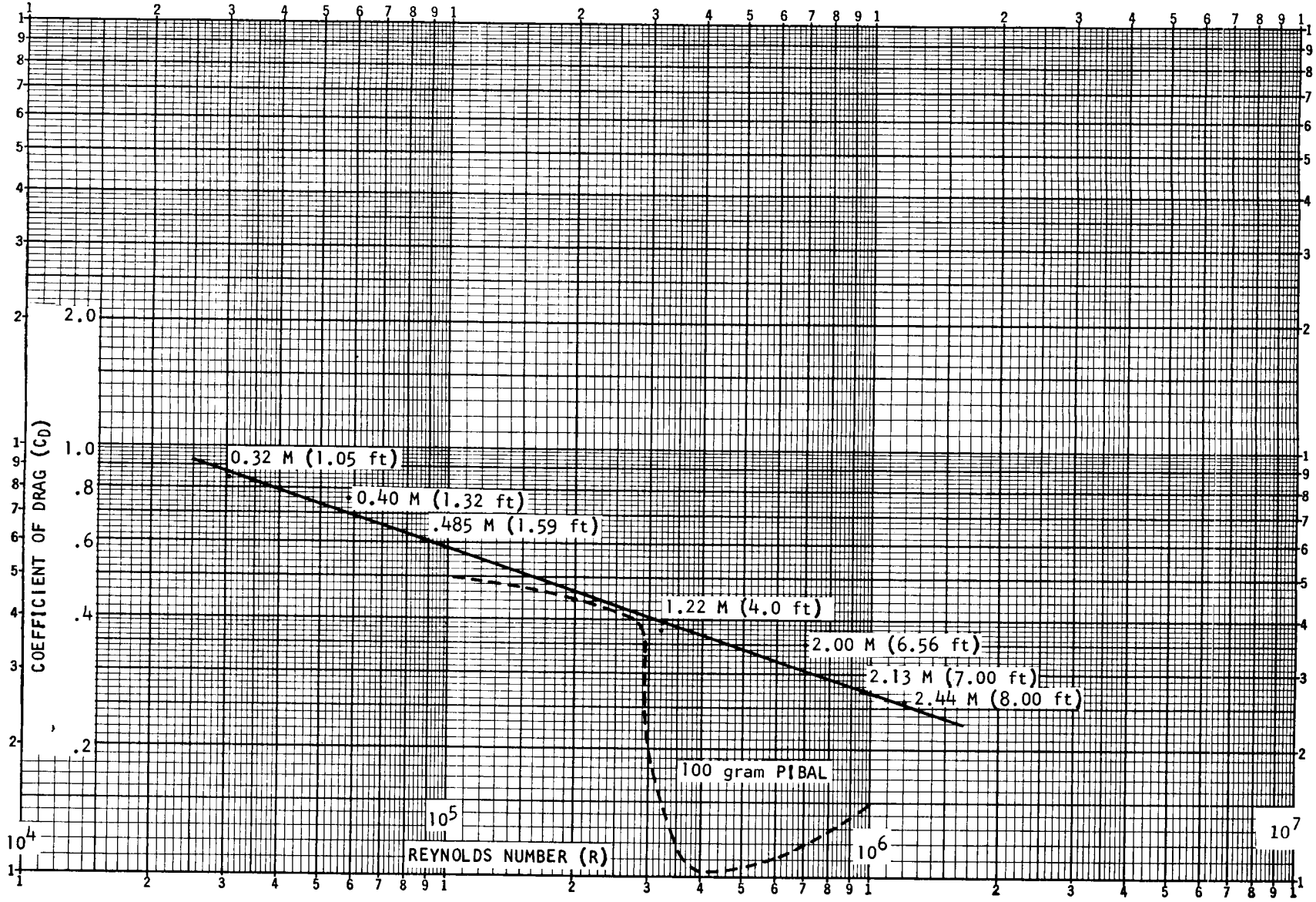

Figure 3. Coefficient of Drag (C_D) vs. Reynolds Number (R) for Various Balloon Diameters

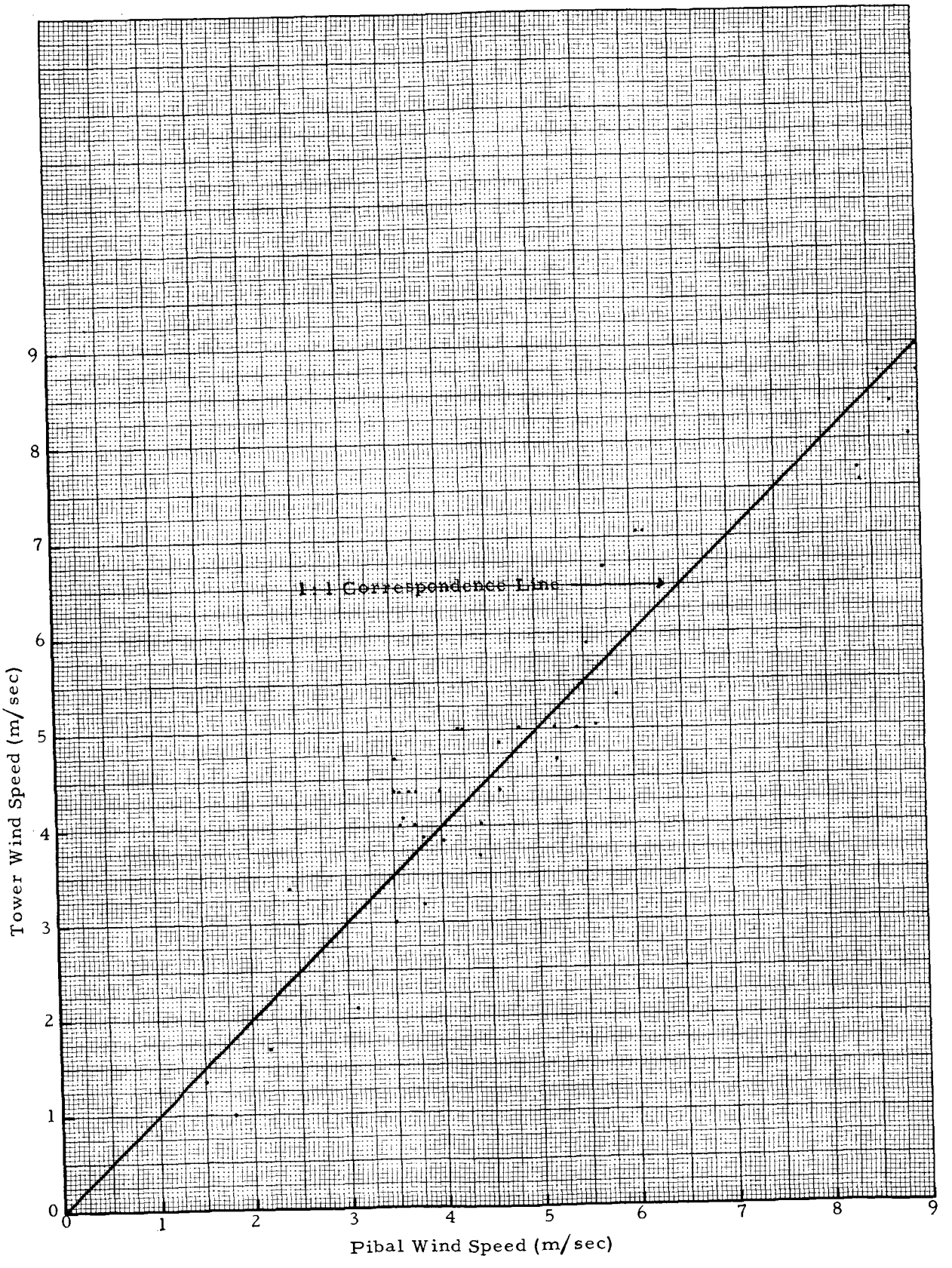

Figure 4. Tower/Pibal Wind Speed Comparison

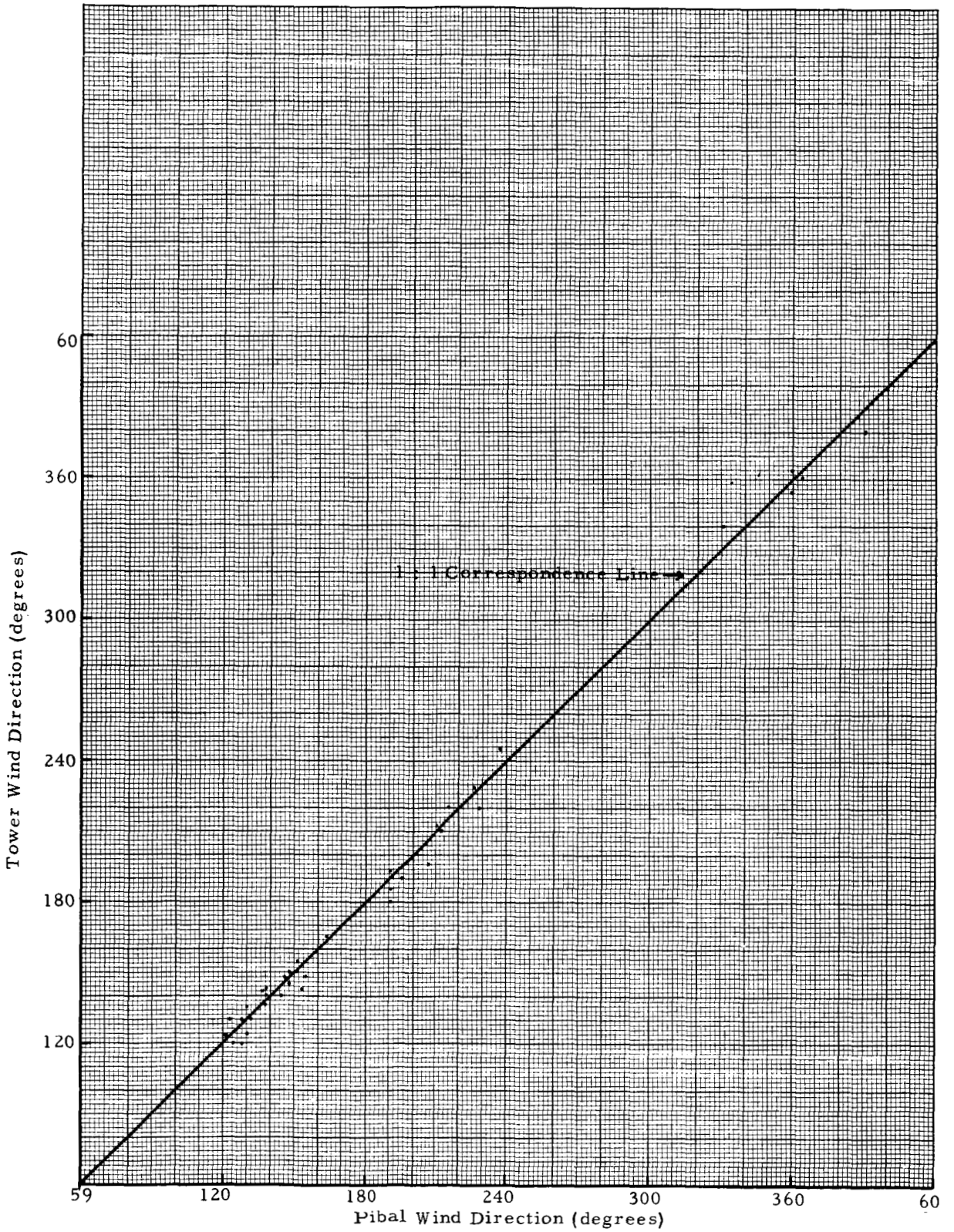

Figure 5. Tower/Pibal Wind Direction Comparison

TABLE I

Comparison of Reynolds Number (R) versus Drag Coefficients (C_D) for Various Sphere Diameters (d) at Approximate Sea Level Pressures

Diameter	m (ft)	C_D	R x 10^5	Remark
0.320	(1.05)	.82	0.31	PIBAL (10 gm)
0.403	(1.32)	.77	0.58	PIBAL (10 gm)
0.485	(1.59)	.60	0.87	PIBAL (10 gm)
1.22	(4.00)	.38	3.25	ROSE TYPE
1.01	(3.31)	.36	3.31	PIBAL (100 gm)
2.00	(6.56)	.35	7.00	ROSE (Standard)
2.13	(7.00)	.28	9.50	ROSE TYPE
2.44	(8.00)	.26	12.00	ROSE TYPE

TABLE II

Tower/Pibal Wind Comparison at 15.24 m, MSFC, Huntsville, Alabama

Date	Observation	Wind Direction (deg)			($m\ sec^{-1}$)			Horizontal Distance Displacement (m)
		Tower	Pibal	Difference	Tower	Pibal	Difference	
Oct. 4, 1966	1	220	215	5	1.00	1.18	-0.18	1.7
Oct. 4, 1966	2	185	190	-5	1.34	1.51	-0.17	3.7
Oct. 4, 1966	3	228	226	2	2.12	3.08	-0.96	4.9
Oct. 6, 1966	6	020	030	-10	1.67	2.17	-0.50	3.5
Oct. 6, 1966	8	360	003	-3	5.03	5.42	-0.39	2.5
Oct. 6, 1966	9	003	355	8	3.01	3.01	0.00	2.0
Oct. 6, 1966	10	340	331	9	4.09	3.60	0.49	3.4
Oct. 6, 1966	11	354	359	-5	4.02	4.40	-0.38	5.4
Nov.17, 1966	3	196	206	-10	3.85	4.02	-0.17	3.2
Nov.17, 1966	16	212	210	2	5.36	5.82	-0.46	4.9
Nov.17, 1966	17	210	212	-2	4.02	3.73	0.29	4.2
Nov.17, 1966	18	193	190	3	4.85	4.61	0.24	4.1
Jan.31, 1967	11	220	228	-8	4.36	3.51	0.85	2.8
Jan.31, 1967	12	245	237	8	7.59	8.38	-0.79	3.9
Mar.30, 1967	5	124	130	-6	7.71	8.36	-0.65	0.4
Mar.30, 1967	10	135	130	5	7.04	6.06	0.98	2.7
Mar.30, 1967	11	140	138	2	8.72	8.99	-0.27	2.6
Mar.30, 1967	15	143	138	5	8.38	8.72	-0.34	2.6
Mar.30, 1967	16	148	146	2	7.04	6.13	0.91	4.4
Mar.30, 1967	19	120	128	-8	8.72	8.58	0.14	2.5
Mar.30, 1967	23	130	132	-2	5.03	5.61	-0.58	0.4
Mar.30, 1967	29	120	124	-4	8.05	8.89	-0.84	0.2
Mar.31, 1967	38	190	195	-5	4.02	3.56	0.46	5.0
Mar.31, 1967	39	180	190	-10	4.35	3.67	0.68	3.6
Mar.31, 1967	42	190	195	-5	4.36	3.98	0.38	4.4

TABLE II (Continued)

Date	Observation	Wind Direction(deg)			(m sec^{-1})			Horizontal Distance Displacement (m)
		Tower	Pibal	Difference	Tower	Pibal	Difference	
June 28, 1967	4	155	151	4	4.36	4.60	-0.24	4.5
June 28, 1967	10	165	163	2	3.88	3.78	0.10	5.0
June 28, 1967	11	140	145	-5	3.69	4.39	-0.70	1.7
June 28, 1967	13	136	138	-2	3.17	3.78	-0.61	5.0
June 28, 1967	14	142	137	5	3.36	2.43	0.93	3.1
June 28, 1967	15	145	148	-3	5.03	5.17	-0.14	2.4
June 28, 1967	16	150	151	-1	5.03	4.19	0.84	2.8
June 28, 1967	18	148	155	-7	4.36	3.55	0.81	2.3
June 28, 1967	20	150	148	2	5.03	4.82	0.21	3.9
June 28, 1967	21	140	144	-4	4.36	3.73	0.63	4.6
June 28, 1967	22	123	121	2	5.90	5.54	0.36	6.4
June 28, 1967	24	130	123	7	4.70	5.20	-0.50	3.7
June 28, 1967	30	130	128	2	4.68	3.52	1.16	5.8
June 28, 1967	31	140	145	-5	6.71	5.73	0.98	5.3
June 28, 1967	36	143	153	-10	5.03	4.21	0.82	5.8

APPENDIX A

Aerodynamic Drag Coefficient

The aerodynamic drag coefficient was calculated as follows: The buoyant force (F_B) of the balloon is defined by the equation:

$$F_B = g[vol(\rho_a - \rho_g) - M_B] \tag{1}$$

where the following notations are defined:

g = gravitational acceleration

vol = volume of sphere

ρ_a = ambient air density

ρ_g = density of helium gas

M_B = mass of balloon.

The drag coefficient (C_D) was determined from the equation,

$$C_D = \frac{F_B}{\frac{1}{2}\rho_a \text{ A ref } V^2} \tag{2}$$

where A ref is the cross-sectional area and V is the vertical rise rate of the balloon. The drag coefficient for spheres or cylinders are greatly affected by R. R is the ratio of the inertial force to viscous forces and is given by

$$R = \frac{Vd}{\nu} \tag{3}$$

where V is the vertical rise rate of the balloon, d is the balloon diameter, and ν is the kinematic viscosity.

APPENDIX B

Mathematical Derivations

The total horizontal velocity V_t was computed from the X and Y coordinates of horizontal projection of the trajectory as determined from the azimuth and elevation angles and the distance D between the two cameras.

The horizontal coordinates X and Y are computed from the equations listed below.

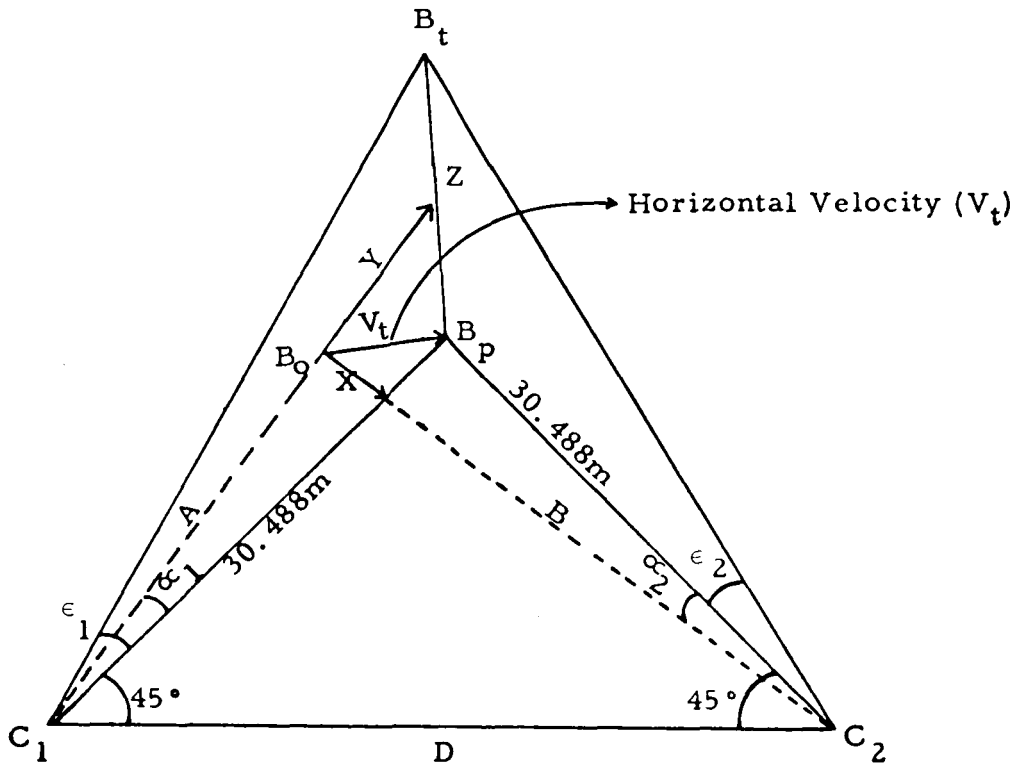

Horizontal Distance Diagram

Symbols

C_1	position of the south camera
C_2	position of the east camera
α_1 and ϵ_1	azimuth and elevation angles from C_1 camera

α_2 and ϵ_2 — azimuth and elevation angles from C_2 camera

B_o — projection of balloon position on horizontal plane through C_1 and C_2 cameras (at time, t)

B_t — balloon position on a horizontal plane through C_1 and C_2 cameras (at time, $t + \tau$).

From the law of sines

$$\frac{B}{\sin(45° + \alpha_1)} = \frac{A}{\sin(45° - \alpha_2)} = \frac{D}{\sin 180° - [(45° + \alpha_1) + (45° - \alpha_2)]} \tag{4}$$

where

$$\sin 180° - [(45° + \alpha_1) + (45° - \alpha_2)]$$

is the difference of two angles, $\sin(x - y) = \sin x \cos y - \cos x \sin y$ and is equal to $\cos(\alpha_1 - \alpha_2)$.

The law of sines is simplified to

$$\frac{B}{\sin(45° + \alpha_1)} = \frac{A}{\sin(45° - \alpha_2)} = \frac{D}{\cos(\alpha_1 - \alpha_2)} \tag{5}$$

and

$$A = \frac{D \sin(45° - \alpha_2)}{\cos(\alpha_1 - \alpha_2)} \tag{6}$$

and

$$B = \frac{D \sin(45° + \alpha_1)}{\cos(\alpha_1 - \alpha_2)}. \tag{7}$$

The X and Y components of the horizontal travel distance are

$$X = A \sin \alpha_1 \quad \text{positive east} \tag{8}$$

and

$$Y = A \cos \alpha_1 - 30.488 \quad \text{positive north.} \tag{9}$$

The height equation (Z) is calculated from the equation

$$Z = A \tan \epsilon_1 + C \tag{10}$$

where C is the camera elevation correction.

The total horizontal velocity equation (V_t) is

$$V_t = \frac{\sqrt{\Delta X^2 + \Delta Y^2}}{\Delta_t} \ (\text{m sec}^{-1}) \tag{11}$$

where

ΔX = difference between X values at half second intervals

ΔY = difference between Y values at half second intervals,

which becomes

$$V_t = 2\sqrt{\Delta X^2 + \Delta Y^2} \ . \tag{12}$$

The component wind speeds $\dot{X}_n$ and $\dot{Y}_n$ are computed using the following equations:

$$\dot{X}_n = \frac{X_n - X_{n-1}}{\Delta t_{(n,n-1)}} \quad (\text{m/sec})$$

$$\dot{Y}_n = \frac{Y_n - Y_{n-1}}{\Delta t_{(n,n-1)}} \quad \text{(m/sec)}.$$

The computed wind speeds are associated with the top of the layer designated by n. The direction from which the wind is blowing, ψ_n, is calculated as follows:

$$\psi_n = \tan^{-1} \frac{\dot{X}_n}{\dot{Y}_n} + \text{quadrant correction}.$$

The quadrant correction is determined from the sign of $\dot{X}_n$ and $\dot{Y}_n$ as follows:

$$\left.\begin{matrix}\dot{X}_n + \\ \dot{Y}_n -\end{matrix}\right\} \; 360 - \psi_n$$

$$\left.\begin{matrix}\dot{X}_n + \\ \dot{Y}_n +\end{matrix}\right\} \; 180 + \psi_n$$

$$\left.\begin{matrix}\dot{X}_n - \\ \dot{Y}_n +\end{matrix}\right\} \; 180 - \psi_n$$

$$\left.\begin{matrix}\dot{X}_n - \\ \dot{Y}_n -\end{matrix}\right\} \; \psi_n .$$

REFERENCES

1. Rider, L. J. and M. Armendariz, "A Comparison of Tower and Pibal Wind Measurements," Journal of Applied Meteorology, February 1966.

2. Rider, L. J. and M. Armendariz, "Differences of Tower and Pibal Wind Profiles," ECOM-5095, Atmospheric Sciences Laboratory, White Sands Missile Range, New Mexico, November 1966.

3. Camp, Dennis W., "Preliminary Results of Anemometer Comparison Tests," Aero-Astrodynamics Laboratory, NASA TM X-53451, April 26, 1966.

4. Scoggins, James R., "Sphere Behavior and the Measurements of Wind Profiles," NASA TN D-3994, June 1967.

5. Schlichting, Herman, Boundary Layer Theory, McGraw-Hill Book Co., Inc., New York, 1939.

6. Technical Manual TM11-2405, Department of the Army, dated February 1957.

APPROVAL NASA TM X-53663

WIND COMPARISON ANALYSIS OF PIBAL VERSUS ANEMOMETER

by Michael Susko

The information in this report has been reviewed for security classification. Review of any information concerning Department of Defense or Atomic Energy Commission programs has been made by the MSFC Security Classification Officer. This report, in its entirety, has been determined to be unclassified.

This document has also been reviewed and approved for technical accuracy.

John W. Kaufman

John Kaufman
Acting Chief, Atmospheric Dynamics Branch

W. W. Vaughan

W. W. Vaughan
Chief, Aerospace Environment Division

E. D. Geissler
Director, Aero-Astrodynamics Laboratory

DISTRIBUTION

DIR
R-AERO-DIR
  Dr. Geissler
  Mr. Jean

R-AERO-A
  Mr. Dahm
  Mr. Reed

R-AERO-D
  Mr. Rheinfurth
  Mr. Ryan
  Mrs. King

R-AERO-T
  Dr. Heybey

R-AERO-Y
  Mr. Vaughan (5)
  Mr. Kaufman (10)
  Mr. Fichtl
  Mr. Susko (50)
  Mr. Hill
  Mr. Camp
  Mrs. Alexander
  Mr. R. Smith
  Mr. O. Smith
  Mr. Daniels
  Mr. Turner (5)
  Mr. Hasseltine
  Mr. O. Vaughan

DEP-T
CC-P
I-RM-M
MS-H
MS-IP
MS-IL(8)
MS-T(6)

EXTERNAL

Kennedy Space Center
  Mr. L. Keene, IN-DAT-2
  Mr. R. H. Jones, In-MSD-3

Mr. George Ortiz
NASA, Manned Spacecraft Center
White Sands Missile Range Operations
Post Office Drawer, MM
Las Cruces, New Mexico 88001

Mr. C. W. Hines
NASA, Pacific Launch Office
P. O. Box 425
Lompoc, California 93428

Mr. Gene E. Godwin
Programs and Liaison Branch
NASA, Wallops Station, Virginia 23337

Mr. Manuel Armendariz
U. S. Army
Electronics Research & Development Activity
White Sands Missile Range
Las Cruces, New Mexico 88001

Mr. L. J. Rider
Atmospheric Sciences Laboratory
U. S. Army Electronics Command
White Sands Missile Range
Las Cruces, New Mexico 88001

Dr. J. R. Scoggins
College of Geosciences
Department of Meteorology
College Station, Texas 77843

Meteorology Department
Dugway Proving Ground
Dugway, Utah
Attn: Mr. Paul Carson

Mr. R. K. Jenkins
SELWS-ER
U. S. Army Electronic Research & Development Activity
White Sands Missile Range, New Mexico 88002

Mr. W. L. Webb
SELWS-E
U.S. Army Electronic Research & Development Activity
White Sands Missile Range, New Mexico 88002

DISTRIBUTION (Continued)

Mrs. Norvella Billions
AMSMI-RRA
Redstone, Alabama 35809

Mr. T. R. Carr
Code 3251, Box 22
Pacific Missile Range
Point Mugu, California 93041

Mr. O. H. Daniel
MU-235
Pan American World Airways, Inc.
Air Force Eastern Test Range
Patrick AFB, Florida 32925

LCOL H. R. Montague, USAF
ETZ
Air Force Eastern Test Range
Patrick AFB, Florida 32925

Mr. N. J. Asbridge
WTWU
Air Force Western Test Range
Vandenberg AFB, California 93437

LCOL R. F. Durbin, USAF
WTW
Air Force Western Test Range
Vandenberg AFB, California 93437

Mr. Q. S. Dalton
Code 3069
Naval Ordnance Test Station
China Lake, California 93555

Mr. A. J. Krueger
Code 50
Naval Ordnance Test Station
China Lake, California 93555

LCOL B. F. Walker, USAF
PGLW
Air Proving Ground Center
Eglin AFB, Florida 32542

Cdr. W. S. Houston, Jr., USN
Chief, Environmental Science Div.
Office of Asst Dir (Rsch)
OSD/Dept of Defense Rsch & Engr
Room 3E-1037, Pentagon
Washington, D. C. 20301

Mr. John F. Spurling
Head, Aeronomy & Applications Ofc
Range Engineering Division
NASA, Wallops Station
Wallops Island, Virginia 23337

Mr. R. E. McGavin, 520.80
Tropospheric Telecommunications Lab
Inst for Telecom Sciences & Aeronomy
Environmental Science Services Admin
Boulder, Colorado 80302

Mr. C. J. Callahan
FC-3
Deputy, Fedl Coordinator for Met
Services & Supporting Rsch
U.S. Department of Commerce
Environmental Science Services Adm
Washington, D. C. 20235

Maj R. I. Vick, USAF
PGGW
Air Proving Ground Center
Eglin AFB, Florida 32542

LCOL I. A. Van Brunt, USAF
WEA
Air Force Flight Test Center
Edwards AFB, California 93523

LCOL D. E. McPherson, Jr.
SSOTW
Air Force Satellite Control Facility
Sunnyvale, California 94086

LCOL C. J. Loisel
SSSW
Hq, Space Systems Division
Los Angeles AF Station
Los Angeles, California 90045

Mr. K. C. Steelman
AMSEL-RD-SM
U.S. Army Electronic Research & Development Laboratory
Fort Monmouth, New Jersey 07703

Mr. H. D. Bagley
AMSMI-RRA, Bldg. 5429
Physical Science Laboratory
Redstone Arsenal, Alabama 35809

Mr. A. L. Miller
AIR-5403
Naval Air Systems Command
Washington, D. C. 20360

Mr. R. M. Fenn
KXR, DoD Code 1232
U.S. Naval Weapons Laboratory
Dahlgren, Virginia 22448

Mr. H. Demboski
Code 421
Office of Naval Research
Washington, D. C. 20360

Cdr T. H. R. O'Neill USN
Naval Weather Station
Code 70
Washington (Navy Yard Annex)
Washington, D. C. 20390

Maj W. D. Kleis, USAF
SCWT
Air Force Systems Command
Andrews AFB, Maryland 20331

LCOL F. J. Franz, USAF
BSOW
Ballistics Systems Division
Norton AFB, California 92409

LCOL J. M. Dunn
National Range Division (NRX)
Patrick AFB, Florida 32925

Mr. R. Leviton
CRER
Air Force Cambridge Rsch Lab
L. G. Hanscom Field
Bedford, Massachusetts 01731

Mr. V. S. Hardin
AWSAE
Air Weather Service
Scott AFB, Illinois 62226

Mr. W. C. Spreen
Code SA
Hq, National Aeronautics and Space Administation
Washington, D. C. 20546

Mr. H. B. Tolefson
NASA, Langley Research Center
Mail Stop 240
Hampton, Virginia 23365

Mr. K. M. Nagler
Chief, Space Operations Support Div
U.S. Weather Bureau, ESSA
Silver Spring, Maryland 20910

Mr. C. A. Olson
Code 7261
Sandia Corp., Sandia Base
Albuquerque, New Mexico 87110

Mr. L. B. Smith
Code 5241
Sandia Corporation
Albuquerque, New Mexico 87110

Mr. Lee L. Sims
USAERDAA, Meteorology Dept.
U.S. Army Electronics Proving Gd
Ft. Huachuca, Arizona 85613

Scientific & Technical Inf. Facility (25)
Attn: NASA Rep. S-AK/RKT
P.O. Box 33
College Park, Md. 20740